

## Geological investigations of the Wasekwan Lake area, Lynn Lake greenstone belt, northwestern Manitoba (parts of NTS 64C10, 15)

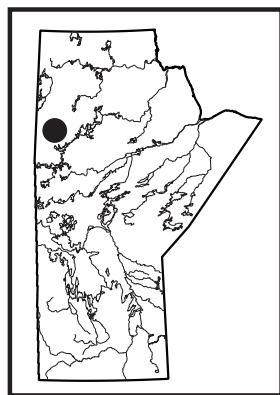
by X.M. Yang and C.J. Beaumont-Smith

### In Brief:

- New detailed mapping provides an updated geological context for gold mineralization in the Johnson shear zone
- Important controls on Au mineralization include structural and chemical traps along contacts between map units of contrasting rheology
- Granitoid intrusions locally provide an empirical guide to mineralization

### Citation:

Yang, X.M. and Beaumont-Smith, C.J. 2017: Geological investigations of the Wasekwan Lake area, Lynn Lake greenstone belt, northwestern Manitoba (parts of NTS 64C10, 15); *in* Report of Activities 2017, Manitoba Growth, Enterprise and Trade, Manitoba Geological Survey, p. 117–132.



### Summary

In 2017, the Manitoba Geological Survey continued a multiyear bedrock mapping project in the Paleoproterozoic Lynn Lake greenstone belt. Detailed mapping at 1:20 000 scale focused on the southern supracrustal belt in the Wasekwan Lake area to resolve questions regarding the geological context of Au mineralization and support ongoing exploration activity in the vicinity of the Burnt Timber Au deposit. This detailed mapping also aligns with the broader objectives of the project, which are to constrain the complex geology and geodynamic evolution of the Lynn Lake greenstone belt, and to identify key factors controlling the formation of its diverse mineral deposits (e.g., orogenic Au, magmatic Ni-Cu-PGE, volcanogenic massive-sulphide Cu-Zn).

Preliminary mapping indicates that the area is dominantly underlain by massive to pillowed basalt, with minor basaltic andesite, dacite, rhyolite and related volcanoclastic rocks, along with subordinate sedimentary rocks. The volcanic sequence is spatially and temporally associated with reworked volcanoclastic and epiclastic rocks, as well as banded iron formation (BIF), features suggestive of deposition in a setting comparable to modern volcanic arcs or back-arc basins. These supracrustal rocks are intruded by various granitoid intrusions, in addition to being overprinted by multiple phases of deformation and metamorphism.

Additional findings from the 2017 field season include: 1) Au mineralization appears to be spatially associated with structural contacts between volcanoclastic rocks (unit 1), Fe-rich mafic volcanic rocks (unit 2) and sedimentary rocks (unit 3) that occur along, or adjacent to, the Johnson shear zone and associated structures, which may have created traps (structural and chemical) for Au-bearing fluids; 2) the presence of garnet-hornblende porphyroblasts well preserved in feldspathic greywacke (unit 3), that suggests it, together with the other supracrustal rocks, may have experienced middle-amphibolite facies metamorphism, although the presence of actinolite–tremolite and sodic plagioclase in mafic volcanoclastic rocks (unit 1) indicates that they have been subject to greenschist-facies retrograde overprint; 3) gabbroic intrusions of unit 4 may have potential to host magmatic Ni-Cu-Co-(Pt) mineralization but require further evaluation; and 4) late granitic porphyry dikes (unit 7) and granitoid plutons (unit 6) need to be investigated for their potential connection to Au mineralization.

### Introduction

The Manitoba Geological Survey initiated a detailed bedrock mapping project in the Paleoproterozoic Lynn Lake greenstone belt (LLGB) of northwestern Manitoba (Figure GS2017-11-1) in 2015. The broader objectives of this project are to compile all available information and produce an up-to-date synthesis for the belt to accompany a seamless series of 1:50 000 scale maps covering nine NTS sheets. Thus far, fieldwork has been focused around the past-producing MacLellan and Farley Lake Au deposits, with emphasis on investigating their geology and geodynamic evolution as they relate to the Au metallogeny of the belt. In addition, key factors controlling the formation of various types of mineral deposits are being reviewed (e.g., orogenic Au, magmatic Ni-Cu-PGE, volcanogenic massive-sulphide Cu-Zn). These new bedrock geological maps incorporate litho-geochemistry, radiogenic-isotope analysis and a GIS compilation of historical data.

Detailed mapping at a scale of 1:20 000 in the summer of 2017 focused on the Wasekwan Lake area, particularly around the Burnt Timber (BT) Au deposit. The BT deposit occurs within the Johnson shear zone (JSZ; Figure GS2017-11-1; Peck et al., 1998; Jones, 2005; Jones et al., 2006) and displays significant differences to the MacLellan and Farley Lake deposits, which are hosted in the regionally extensive Agassiz metallotect (Figure GS2017-11-1; Fedikow and Gale, 1982; Fedikow, 1992; Ma et al., 2000; Ma and Beaumont-Smith, 2001; Park et al., 2002; Yang and Beaumont-Smith, 2015a, 2016a, b). Understanding these differences will provide important constraints for understanding the Au metallogeny of the Lynn Lake belt. In addition, gabbroic intrusions (e.g., Cockeram



Lake intrusion) in the map area are petrologically similar to the Lynn Lake gabbroic intrusion that hosts the Lynn Lake magmatic Ni-Cu-Co mine (Pinsent, 1980; Jurkowski, 1999; Yang and Beaumont-Smith, 2015a, b), suggesting that the Wasekwan Lake area also has potential for this type of deposit.

The preliminary map (Yang and Beaumont-Smith, 2017) associated with this report is generated from 279 field stations (this study), compiled historical data (138 stations from Gilbert et al., 1980; 84 stations from C.J. Beaumont-Smith, unpublished data, 2006) and detailed airborne electromagnetic-survey data provided by Carlisle Goldfields Ltd. (now Alamos Gold Inc.).

## Regional geology

The LLGB (Bateman, 1945) is an important tectonic element of the Reindeer zone of the Trans-Hudson orogen (Stauffer, 1984; Lewry and Collerson, 1990), which is the largest Paleoproterozoic orogenic belt of Laurentia (Hoffman, 1988; Corrigan et al., 2007, 2009). The LLGB is bounded to the north by the Southern Indian domain, a mixed metasedimentary and metaplutonic domain; to the south, it is bounded by the Kiseynew metasedimentary domain (Gilbert et al., 1980; Syme, 1985; Zwanzig et al., 1999; Beaumont-Smith and Böhm, 2004). Similar Paleoproterozoic greenstone belts also occur to the east (Rusty Lake belt), to the west (La Ronge belt) and to the far south (Flin Flon belt; e.g., Ansdell et al., 1999; Ansdell, 2005; Corrigan et al., 2007, 2009).

The LLGB consists of two east-trending, steeply dipping belts that contain various supracrustal rocks of the Wasekwan group (Bateman, 1945; Gilbert et al., 1980), along with younger molasse-type sedimentary rocks of the Sickle group (Figure GS2017-11-1; Norman, 1933). The southern and northern belts are separated by granitoid plutons of the Pool Lake intrusive suite (Figure GS2017-11-1; Gilbert et al., 1980; Baldwin et al., 1987) which are divided into pre- and post-Sickle intrusions based on their temporal relationships to the Sickle group. In the central and southern parts of the LLGB, the Sickle group overlies the Wasekwan group and felsic–mafic plutonic rocks of the Pool Lake intrusive suite along an angular unconformity. The Sickle group correlates well with the 1850–1840 Ma MacLellan group in the La Ronge greenstone belt in Saskatchewan in terms of composition, stratigraphic position and contact relationships (Ansdell et al., 1999; Ansdell, 2005), although it could be as old as 1865 Ma, based on regional correlations in the Trans-Hudson orogen (Corrigan et al., 2007, 2009). Cutting the entire belt are the much younger Mackenzie dikes (ca. 1267 Ma; Baragar et al., 1996), indicated by regional aeromagnetic data.

The northern Lynn Lake belt consists mostly of subaqueous, tholeiitic, mafic metavolcanic and metavolcaniclastic rocks interpreted as an overall north-facing, steeply dipping succession that occupies the upright limb of a major antiformal structure (Gilbert et al., 1980). Included in the northern belt is the Agassiz metallotect (Fedikow and Gale, 1982; Fedikow, 1986, 1992), a relatively narrow, stratigraphically and structurally distinct entity consisting of ultramafic flows (picrite), banded oxide-facies iron formation and associated exhalative

and epiclastic rocks (Ma et al., 2000; Ma and Beaumont-Smith, 2001; Park et al., 2002). The Agassiz metallotect contains Au mineralization (Figure GS2017-11-1) and intense deformation fabrics (Beaumont-Smith and Böhm, 2004). The northern belt is unconformably overlain to the north by marine conglomerate and turbiditic sedimentary rocks, known as the Ralph Lake conglomerate and Zed Lake greywacke, respectively (Gilbert et al., 1980; Manitoba Energy and Mines, 1986; Zwanzig et al., 1999). This clastic succession is derived largely from the Wasekwan group and plutonic rocks, with the majority of detrital zircons returning ca. 1890 Ma ages (Beaumont-Smith and Böhm, 2004).

The southern belt consists largely of subaqueous tholeiitic to calcalkalic metavolcanic and metavolcaniclastic rocks, including minor amounts of metabasalt with geochemical signatures comparable to modern mid-ocean–ridge basalt. The tholeiitic to calcalkalic rocks include older (ca. 1890 Ma) contaminated-arc rocks, as well as younger (ca. 1855 Ma) juvenile-arc volcanic rocks (Peck and Smith, 1989; Zwanzig et al., 1999; Zwanzig, 2000; Beaumont-Smith and Böhm, 2003, 2004). Structural analysis of the LLGB suggests that it is highly transposed (Beaumont-Smith and Rogge, 1999; Beaumont-Smith and Böhm, 2002), calling into question previous stratigraphic and structural interpretations.

Significant differences in the geology and geochemistry of the northern and southern belts reflect this complex structural scenario and/or regional differences in tectonic setting (Syme, 1985; Zwanzig et al., 1999). This complexity leads to the suggestion that the term ‘Wasekwan group’ should be abandoned because it contains the diverse volcanic assemblages structurally juxtaposed in the evolution of LLGB (see Zwanzig et al., 1999) and thus may represent a tectonic collage similar to that described in the Flin Flon greenstone belt (e.g., Stern et al., 1995). However, this report and accompanying preliminary map (Yang and Beaumont-Smith, 2017) retain the term ‘Wasekwan group’ to maintain consistency with previous LLGB-related literature.

## Geology of the Wasekwan Lake area

The Wasekwan Lake area is located in the southern belt of the LLGB (Figure GS2017-11-1) and consists dominantly of the Wasekwan group supracrustal rocks intruded by plutons of the Pool Lake intrusive suite (Figure GS2017-11-2). Following the convention of previous workers (e.g., Beaumont-Smith and Böhm, 2004), intrusions cutting the Wasekwan group (i.e., the Pool Lake intrusive suite of Gilbert et al., 1980) and those cutting the Sickle group are called, respectively, the pre-Sickle and post-Sickle (e.g., Milligan, 1960) suites; both are cut by a late intrusive suite (Yang and Beaumont-Smith, 2015a, b), identified in the area of the MacLellan Au mine.

Eight map units, including 15 subunits, were defined during the course of bedrock mapping (Table GS2017-11-1). These map units are described in the following sections and shown in Figure GS2017-11-2 (see Yang and Beaumont-Smith, 2017). The supracrustal rocks in the LLGB were metamorphosed in the greenschist to amphibolite facies (Gilbert et al., 1980;

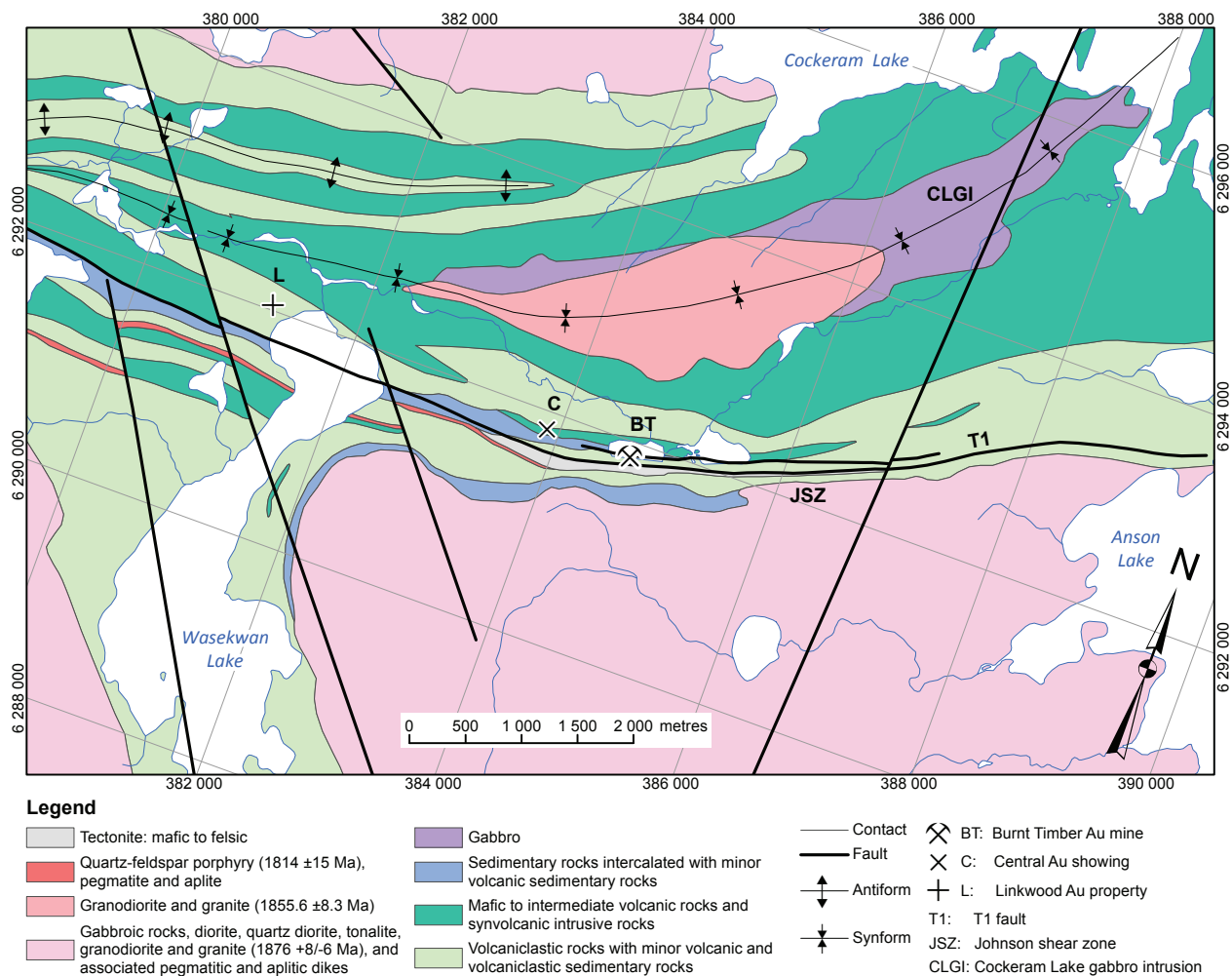


**Figure GS2017-11-2:** Simplified geology of the Wasekwan Lake area, Lynn Lake greenstone belt, northwestern Manitoba (modified from Yang and Beaumont-Smith, 2017).

Beaumont-Smith and Böhm, 2004; Yang and Beaumont-Smith, 2015a, 2016a); however, for brevity, the prefix ‘meta’ is omitted in this report.

**Volcaniclastic rocks with minor volcanic rocks and volcanic sedimentary rocks (unit 1)**

Rocks of unit 1 are widespread in central, southwestern and western parts of the map area (Figure GS2017-11-2). Unit 1 consists mainly of mafic volcaniclastic rocks and lesser amounts of intermediate to felsic volcanic and volcaniclastic rocks that in places appear to have been reworked by sedimentary processes. The volcaniclastic rocks of unit 1 include mafic breccia, tuff breccia, lapillistone, lapilli tuff and tuff, and minor intermediate to felsic lapilli tuff and tuff (Table GS2017-11-1).

Despite being less abundant, outcrops of strongly foliated dacite and rhyolite (subunit 1a) are significant in terms of correlation to similar rocks in the northern belt. Subunit 1a is mainly exposed in the central and west-central portions of the map area (Figure GS2017-11-2). These felsic to intermediate rocks

are very fine grained, pale grey to white on weathered surfaces and light to medium grey on fresh surfaces, and preserve primary features (i.e., flow banding, porphyritic texture) despite being strongly foliated and recrystallized (Figure GS2017-11-3a). Porphyritic dacite and rhyolite contain equant or sub-rounded quartz (0.5–1.3 mm) and locally subhedral to euhedral K-feldspar (0.5–1.5 mm) phenocrysts embedded in a very fine grained to aphanitic groundmass. Locally associated with these rocks is disseminated pyrite and mesoscopic hydrothermal alteration represented by an assemblage of amphibole (actinolite?), chlorite, sericite and carbonate, manifested by dark bluish patches and/or zones up to 20 cm in width that gradually transition to less-altered felsic to intermediate volcanic rocks. It is not uncommon that boudinaged vein quartz occurs along the main S<sub>2</sub> foliation planes (note that the structural terms used in this report follow those in Beaumont-Smith and Böhm, 2003, 2004), some of which contains fine-grained pyrite grains.

Felsic volcaniclastic rocks are less abundant than dacite and rhyolite rocks (subunit 1a). They consist primarily of felsic lapilli tuff that contains very fine to fine-grained rhyolite to

**Table GS2017-11-1:** Lithostratigraphic units of the Wasekwan Lake area, Lynn Lake greenstone belt, northwestern Manitoba.

Unit <sup>1</sup>	Rock type	Affiliation
8	Tectonite: mafic to felsic in composition	Tectonite
<i>Structural contact</i>		
7	Quartz-feldspar porphyry (1814 ±15 Ma <sup>2,4</sup> ), pegmatite and aplite	Late intrusive suite
<i>Intrusive contact</i>		
6	Granodiorite and granite (1855.6 ±8.3 Ma <sup>4</sup> )	
6a	Granodiorite	Post-Sickle intrusive suite
6b	Granite	
<i>Intrusive contact</i>		
5	Gabbroic rocks, diorite, quartz diorite, tonalite, granodiorite, and granite (1876 +8/-6 Ma <sup>3</sup> ) and associated pegmatitic and aplitic dikes	
5a	Tonalite, granodiorite and granite and associated pegmatitic and aplitic dikes	Pre-Sickle intrusive suite
5b	Diorite, quartz diorite and minor gabbroic rocks	
4	Gabbro	
<i>Structural contact</i>		
3	Sedimentary rocks intercalated with minor volcanic sedimentary rocks	
3a	Argillite and greywacke	
3b	Banded iron formation	
3c	Volcanic mudstone and arenite	
<i>Structural contact</i>		
2	Mafic to intermediate volcanic rocks and synvolcanic intrusive rocks	
2a	Diabase and gabbro	
2b	Porphyritic basaltic andesite	Wasekwan group
2c	Plagioclase-phyric basalt and aphyric basalt	
2d	Pillow basalt	
<i>Structural contact</i>		
1	Volcaniclastic rocks with minor volcanic rocks and volcanic sedimentary rocks	
1a	felsic to intermediate volcanic and volcaniclastic rocks	
1b	Intermediate lapilli tuff and tuff	
1c	Mafic lapillistone, mafic lapilli tuff, tuff and minor mafic mudstone	
1d	Mafic tuff breccia and breccia	
?		

<sup>1</sup> on Preliminary Map PMAP2017-3 (Yang and Beaumont-Smith, 2017)

<sup>2</sup> Jones (2005)

<sup>3</sup> Baldwin et al. (1987)

<sup>4</sup> C.J. Beaumont-Smith, unpublished data, 2006

dacite (elongated, subangular to irregular shape; 4–10 mm), feldspar and quartz crystal fragments (2–3 mm) in a tuff matrix that contains lithic (1–2 mm) and mineral fragments (<2 mm; plagioclase, K-feldspar, quartz and biotite).

Intermediate lapilli tuff and tuff (subunit b) typically display millimetre- to centimetre- scale layers, interpreted to represent beds even though they are foliated and, in places, folded. Lapilli tuff contains elongated lithic fragments up to 6 cm in diameter of variable composition (e.g., diorite, rhyolite, porphyritic andesite, aphanitic basalt) that are embedded in a fine-grained matrix consisting of amphibole, biotite, chlorite, epidote, plagioclase and aphanitic material. In places, alternating ~0.5–1 cm thick, dark grey and pale yellow-grey layers

represent mafic and intermediate–felsic intercalations. Lapilli tuff appears to grade laterally to fine-grained tuff that contains interbedded mafic and felsic laminae (~0.5–2 mm), and in which larger lapilli-sized lithic fragments are rare or absent. Some tuff and lapilli tuff are moderately to strongly magnetic due to the presence of scattered, euhedral to subhedral magnetite porphyroblasts (up to 1%; 0.5–2 mm). Noteworthy are plagioclase crystal tuff and lapilli tuff, with thin felsic layers up to 1 cm thick (Figure GS2017-11-3b) that contain a large amount of plagioclase fragments of varied shape (e.g., angular, irregular) ranging in size from 0.1 to 10 mm across, and which are unevenly distributed at the outcrop scale. This feature distinguishes the plagioclase crystal tuff and lapilli tuff from plagioclase-phyric

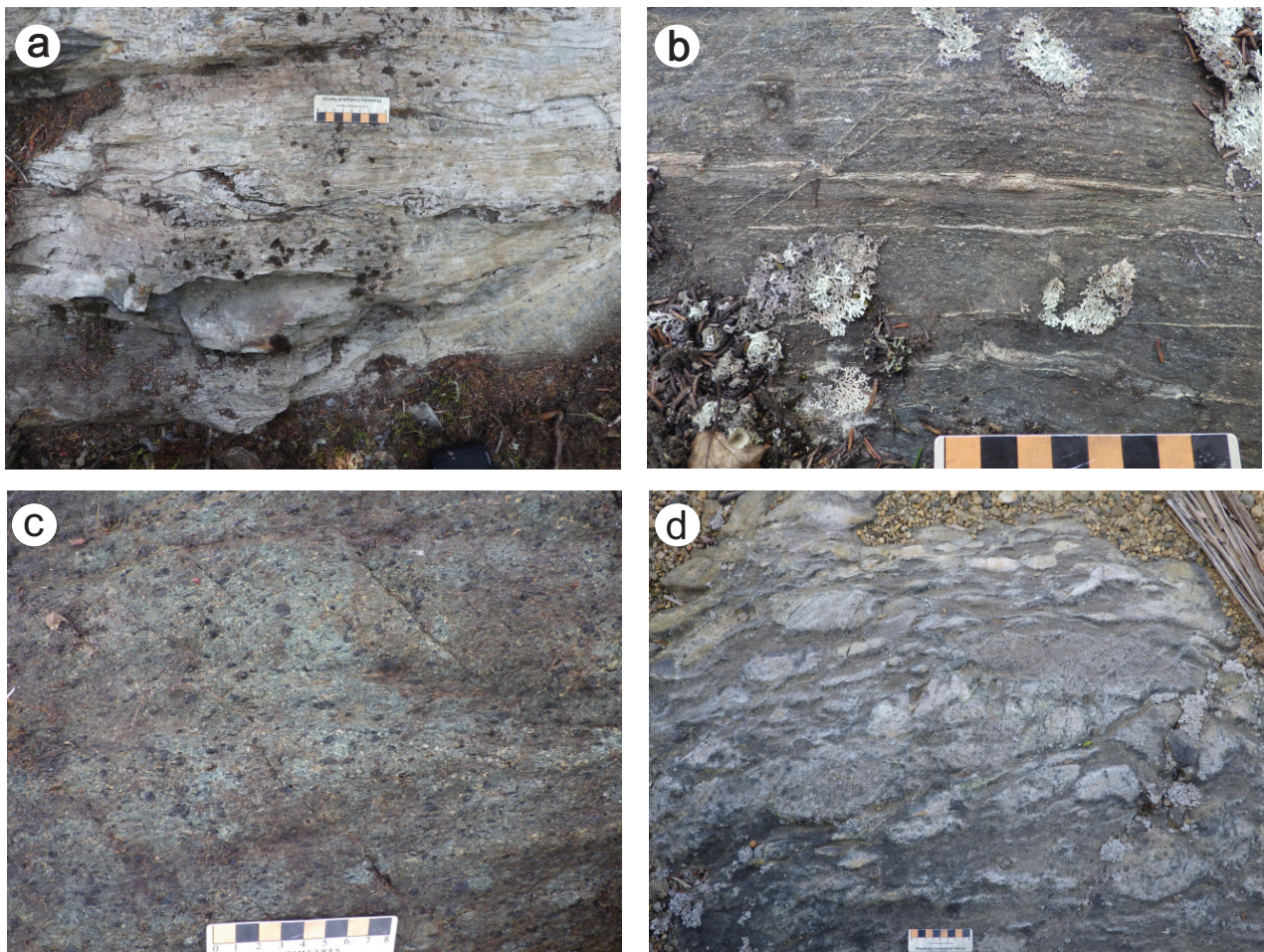


**Figure GS2017-11-3:** Field photographs of unit 1 volcaniclastic rocks with minor volcanic and volcanic sedimentary rocks of the Wasekwan group: **a)** strongly foliated felsic to intermediate volcanic rock (subunit 1a; UTM Zone 14N, 380148E, 6292197N, NAD 83) with a boudinaged quartz vein along  $S_2$  foliation plane; asymmetrical fabric indicates sinistral shear sense; **b)** mafic to intermediate plagioclase crystal tuff and lapilli tuff with thin felsic layers (subunit 1b; UTM 381903E, 6290514N); **c)** foliated lapilli tuff to tuff with amphibole (pseudomorph of clinopyroxene) and plagioclase crystal fragments in fine-grained mafic matrix (subunit 1c; UTM 380522E, 6293155N); **d)** mafic tuff breccia and breccia with plagioclase- and amphibole-phyric basalt fragments and blocks in lapilli tuff to tuff matrix (subunit 1d; UTM 380288E, 6292917N).

basalt (see unit 2c of unit 2 described below). Again, pyrite-bearing quartz veins and veinlets are common along or cross-cutting  $S_2$  foliation in these rocks.

Mafic volcaniclastic rocks have been broken into two subunits; subunit 1c consists of minor mafic mudstone, tuff and lapilli-tuff, whereas subunit 1d consists of mafic tuff breccia and breccia (Table GS2017-11-1). Mafic lapillistone, lapilli tuff and tuff (subunit 1c) are characterized by the presence of mafic lithic fragments in a chloritic matrix. Minor greenish grey, very fine grained, thinly-bedded mafic mudstone is also included in subunit 1c (Table GS2017-11-1), which usually weathers light greenish brown to light grey and contains disseminated pyrrhotite and pyrite. Mafic volcaniclastic rocks are commonly epidote altered. Dark green, acicular amphibole (actinolite?) porphyroblasts (up to 5–10 mm) concentrated in foliation or fracture planes in mafic tuff and lapilli tuff are interpreted to have formed by retrograde metamorphism to greenschist facies.

Some outcrops of mafic tuff and lapilli tuff contain 1–2% euhedral magnetite porphyroblasts (1–3 mm) and coincide with very strong magnetic features on aeromagnetic maps.

The mafic lapilli tuff and tuff (subunit 1c) are generally moderate to strongly foliated and range from texturally variable to relatively homogeneous. These rocks consist of varied amounts of aphyric lithic fragments, plagioclase (up to 40%; 0.1–5 mm) and chloritic amphibole pseudomorphs after pyroxene (up to 15%; 0.2–12 mm) in a fine-grained mafic tuff matrix (Figure GS2017-11-3c). Magnetite and amphibole porphyroblasts are evident in places. Mafic lapilli-sized fragments make up <25% of subunit 1c, but can locally account for up to 80% of the rocks, which are thus termed mafic lapillistone.

Subunit 1d consists of moderate to strongly deformed and foliated heterolithic mafic tuff breccia and breccia. Lithic fragments, ranging from 8 to 25 cm in length, include plagioclase-phyric basalt, plagioclase-amphibole-phyric basalt, aphyric

basalt, lapilli tuff, very fine grained andesite and minor rhyolite clasts embedded in a lapilli tuff and tuff matrix (Figure GS2017-11-3d). The basaltic fragments are subrounded to subangular, varying in shape from irregular to rarely ellipsoidal, and have been stretched along the generally east- to southeast-trending foliation ( $S_2$ ). Some of the aphanitic basalt fragments display epidote alteration and others show reaction rims with very fine grained assemblages of chlorite, epidote, sericite and albite. Some porphyritic basalt blocks contain well-preserved plagioclase and amphibole (after pyroxene) phenocrysts, and are moderately to strongly magnetic. Rare pyrrhotite and pyrite disseminations are evident in both the basaltic fragments and the matrix, suggesting that the basaltic magmas may have been sulphide saturated.

Chert and thin layers of BIF or fragments of these rocks are not observed within mafic tuff breccia and breccia of subunit 1d in the Wasekwan Lake area. This is similar to the mafic volcanoclastic rocks in the area of the Farley Lake Au mine (Yang and Beaumont-Smith, 2016a), but contrasts with the mafic volcanoclastic rocks in the area of the MacLellan Au mine, which contain fragments of thinly bedded chert and BIF (see Ma et al., 2000; Yang and Beaumont-Smith, 2015a).

### ***Mafic to intermediate volcanic rocks and synvolcanic intrusive rocks (unit 2)***

Unit 2 volcanic rocks mainly occur in the northeastern and southwestern parts of the map area (Figure GS2017-11-2). The volcanic succession of unit 2 in the Wasekwan Lake area is dominated by plagioclase-phyric and aphyric basalts as well as pillow basalts, with subordinate porphyritic basaltic andesite, and synvolcanic diabase and gabbro dikes (Table GS2017-11-1).

Pillowed basalts (subunit 2d) are well preserved in a low-strain window exposed along the southeastern shore of Cockeram Lake (Figure GS2017-11-2). Pillow size ranges from 30 to 100 cm, with well-preserved selvages up to 5 cm thick, epidote alteration and subrounded to round quartz±carbonate amygdules up to 1.5 cm in diameter that are concentrated along the inner margin (Figure GS2017-11-4a). In some cases, the concentration of amygdules is asymmetrical, which may be an indicator of younging direction. However, fragments of brecciated pillows with abundant quartz±carbonate±feldspar amygdules of varied shape (e.g., subrounded to irregular) and size (1–10 mm) make it difficult to unambiguously determine younging directions. In high-strain areas, such as the northwestern part of Wasekwan Lake, pillows are strongly deformed and contain a penetrative foliation with width to length ratios up to 1:10. Some pillow selvages are still recognizable, and contain stretched vesicles and quartz amygdules that align parallel to  $S_2$  foliation planes (Figure GS2017-11-4b). Notably, layers of very fine grained interpillow chert up to 5 cm thick are present between some of the strongly deformed pillows, reflecting subaqueous hydrothermal activity associated with basalt eruption.

The plagioclase-phyric basalt of subunit 2c is similar to rocks in the northern belt as described in Gilbert et al. (1980) and by Yang and Beaumont-Smith (2015a, 2016a). This

porphyritic basalt weathers greenish grey to dark grey-black and is green to dark grey on fresh surfaces. It comprises varied amounts of plagioclase phenocrysts and glomerocrysts (in the range of 5 to 50% but most commonly 20 to 30%), and rare amphibole phenocrysts (pseudomorphs after pyroxene) in a fine-grained groundmass of plagioclase, amphibole, epidote, chlorite, carbonate and iron-oxide minerals. Amphibole and magnetite porphyroblasts occur rarely in the basalt. The plagioclase phenocrysts are subhedral and commonly equant (0.5–5 mm), although some glomerocrysts or single plagioclase grains are up to 10 mm. The plagioclase-phyric basalt is texturally homogeneous and moderately to strongly foliated; in high-strain zones, relict plagioclase phenocrysts occur as finer recrystallized aggregates aligned along the  $S_2$  foliation. Distinct light greenish grey epidote-altered domains are common. Trace disseminated pyrrhotite and/or chalcopyrite are evident in many outcrops, and pyrite is common in fractures and faults cutting basalt flows.

Porphyritic basaltic andesite (subunit 2b) contains amphibole (±biotite) and lesser amounts of plagioclase phenocrysts in a fine-grained groundmass, although in some cases it lacks plagioclase phenocrysts. Biotite and sericite alteration is a common feature of these rocks. When plagioclase and amphibole phenocrysts coexist in basaltic andesite (subunit 2b), it is difficult to distinguish it from plagioclase-phyric basalt (subunit 2c), although the latter commonly lacks amphibole (±biotite) phenocrysts. In such circumstances, whole-rock geochemistry and mineral chemistry of plagioclase may help distinguish between the rocks.

Massive aphyric basalt (subunit 2c) is also commonly seen in the map area (Figure GS2017-11-4c). Vesicles and quartz±calcite amygdules are present in some outcrops. Variation in vesicle abundance, size and shape in some exposures indicates that the volcanic sequence at the northwestern part of Wasekwan Lake youngs to the south. This basalt is greyish green on weathered surfaces and dark greyish green on fresh surfaces. In most cases, it is aphanitic. Chlorite and epidote alteration is common in the aphyric basalt, as shown by epidote domains, a few centimetres to a metre across. These epidote domains are generally irregular to ovoid, displaying sharp to gradational contacts with the host aphyric basalt though some epidote is fracture controlled as veins or veinlets, similar to those described in Gilbert et al. (1980), Gilbert (1993) and Yang and Beaumont-Smith (2016a).

Synvolcanic diabase and gabbroic rocks usually occur as dikes and small plugs intruded into unit 2 volcanic rocks, and in some cases into unit 1 volcanoclastic rocks. These mafic intrusive rocks are assigned to subunit 2a. The diabase dikes weather greenish grey to medium grey and are medium to dark green on fresh surfaces; they are very fine to medium grained, porphyritic, and moderately to strongly deformed and foliated (Figure GS2017-11-4d). Equant to subhedral plagioclase phenocrysts (up to 10 mm) occur in a fine-grained groundmass of plagioclase, amphibole, chlorite and iron oxides. Generally, the diabase and gabbroic rocks consists of 50–60% amphibole and 40–50% plagioclase. Grain boundaries between phenocrysts

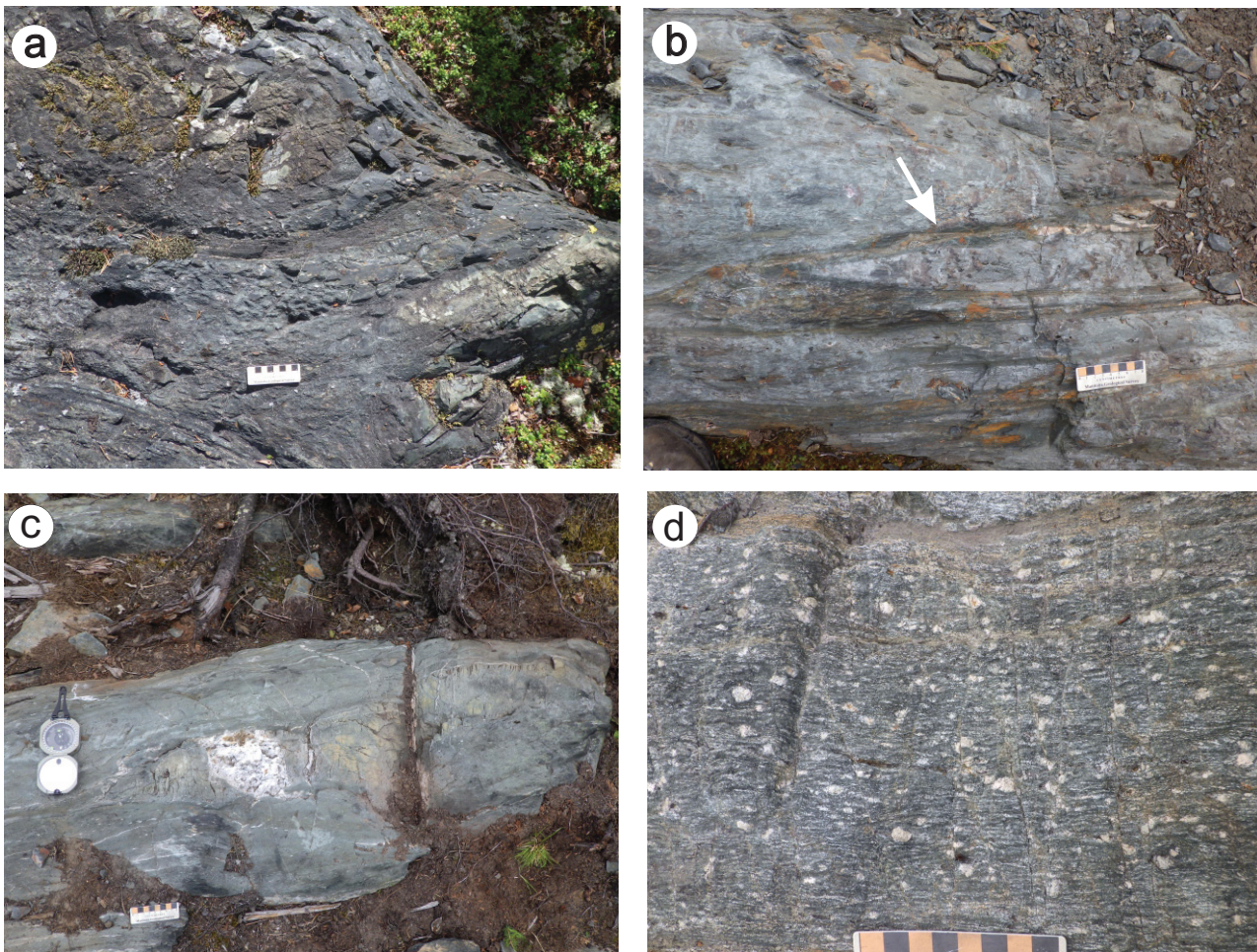


**Figure GS2017-11-4:** Field photographs of mafic to intermediate volcanic rocks and synvolcanic intrusive rocks (unit 2) of the Wasekwan group: **a)** pillow basalt with well-preserved selvage up to 5 cm thick and subrounded quartz±carbonate amygdules (centre right; subunit 2d; UTM Zone 14N, 387265E, 6296232N, NAD83); **b)** strongly deformed and foliated pillow basalt with recognizable selvages (as indicated by arrow) parallel  $S_2$  foliation (subunit 2d; UTM 381153E, 6292415N); **c)** foliated amphibole-phyric basaltic andesite (subunit 2b; UTM 380379E, 6293137N); **d)** very fine grained, foliated, aphyric basalt with epidote-altered domain cut by late quartz veins (subunit 2c; UTM 381146E, 6292386N).

and the groundmass are diffuse due to sericite and chlorite alteration, regardless of the extent of deformation. Disseminated sulphides (e.g., pyrrhotite and/or pyrite; ~0.5–1 mm) are locally evident.

### **Sedimentary rocks intercalated with minor volcanic sedimentary rocks (unit 3)**

Unit 3 sedimentary rocks are subordinate to volcanic and volcanoclastic rocks in the Wasekwan Lake area. The sedimentary rocks are mainly exposed in the central and southwestern portions of the map area (Figure GS2017-11-2). This unit consists of argillite and greywacke (subunit 3a), and BIF (subunit 3b), intercalated with minor volcanic mudstone and arenite (subunit 3c; Table GS2017-11-1).

Quartz feldspathic greywacke and sandstone (subunit 3a) are dominant in the sedimentary succession. The greywacke contains more than 15% clay materials in its matrix, whereas sandstone has much less clays in the matrix. Primary bedding

( $S_0$ ) in the sediments is completely transposed by the regional  $S_2$  foliation. These medium- to coarse-grained greywacke and sandstone are medium tan to yellowish grey on weathered surfaces, and light grey on fresh surfaces. Quartz, feldspar, amphibole and lithic clasts (1.3–2 mm) are angular to subrounded, and well aligned on foliation planes, whereas euhedral to subhedral dark pink garnet (1–3.5 mm) and dark green hornblende (2–3 mm) porphyroblasts are more randomly oriented (Figure GS2017-11-5a, b), albeit that biotite flakes define foliation planes. The mineral assemblage of garnet, hornblende ± biotite in these sedimentary rocks reveals that they have experienced middle-amphibolite facies metamorphism, similar to their counterparts in the northern belt (Yang and Beaumont-Smith, 2015a, 2016a). Scattered sulphide minerals dominated by pyrite are evident in the greywacke and sandstone; in many cases they are associated with quartz veins and veinlets.

In the northeastern part of the Wasekwan Lake area, primary bedding in thin- to medium-bedded argillite and mudstone (subunit 3a) is locally well preserved at the outcrop scale

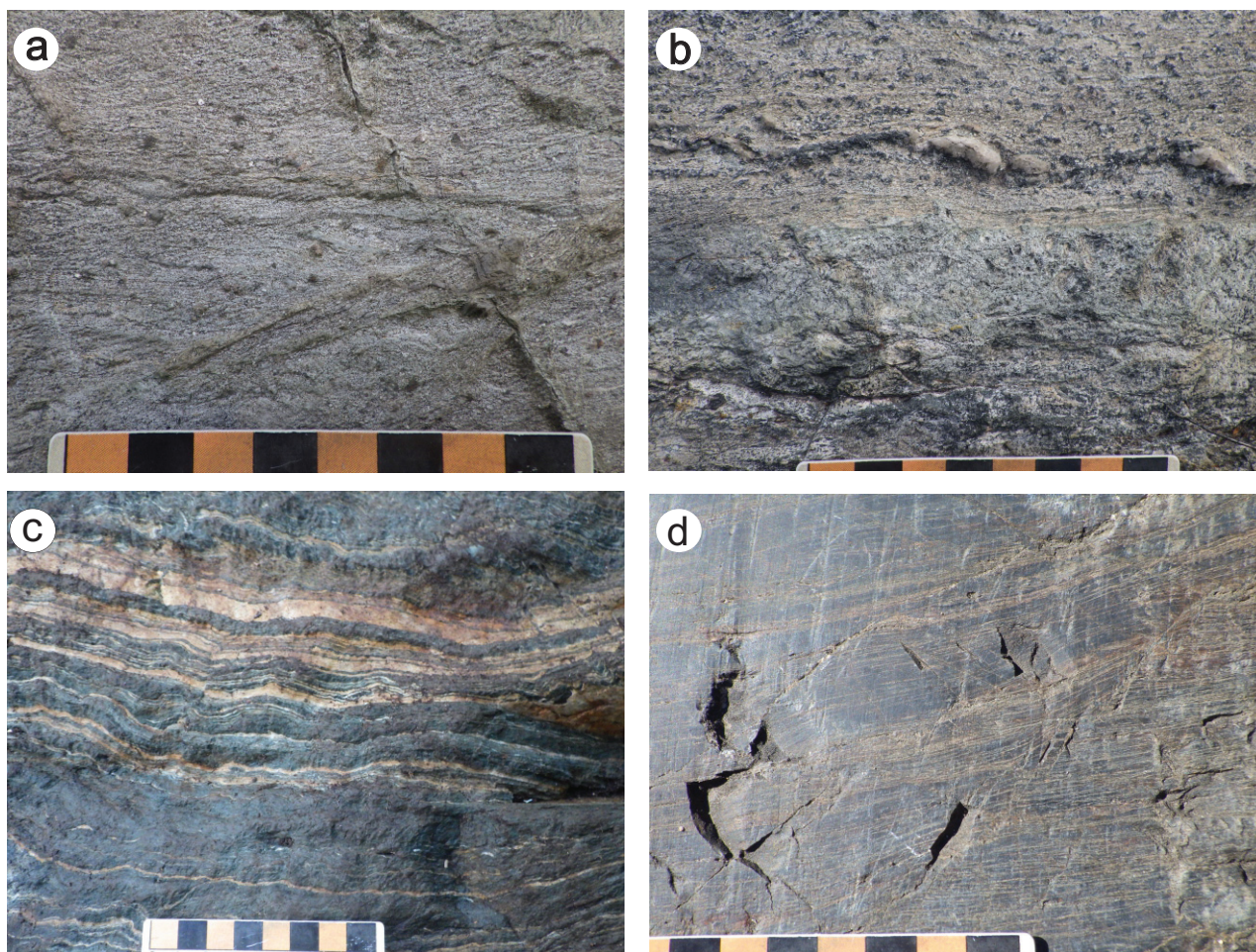


**Figure GS2017-11-5:** Field photographs of sedimentary rocks intercalated with minor volcanic sedimentary rocks (unit 3) of the Wasekwan group: **a)** quartz feldspathic greywacke containing dark pink garnet and hornblende porphyroblasts (subunit 3a; UTM 383443E, 6291886N, NAD 83); **b)** sandstone with hornblende and garnet porphyroblasts, late quartz veinlets occurring along  $S_2$  foliation that has transposed  $S_0$  primary bedding (subunit 3a; UTM 383527E, 6291914N); **c)** thin bedded argillite and mudstone dominated by mafic materials (subunit 3a; UTM 382530E, 6291206N); **d)** banded iron formation consisting of alternating laminae of very fine grained magnetite, biotite-rich mudstone and chert, with bedding transposed by  $S_2$  foliation (subunit 3b; UTM Zone 14N, 384995E, 6291845N).

(Figure GS2017-11-5c), although they are foliated and folded. Millimetre- to centimetre-thick, dark green mafic to light tan felsic layers alternate to form laminae; the mafic laminae are rich in amphibole and chlorite, whereas the felsic laminae contain abundant feldspar and lesser quartz, in addition to minor fine-grained biotite (<0.2 mm) and disseminated pyrite. In a few locations, graded beds indicate that the stratigraphic sequence is younging to the south, consistent with the observed southward younging of mafic volcanic rocks (subunit 2c).

The BIFs (subunit 3b) are rarely exposed southeast of the BT Au deposit (Figure GS2017-11-2), but correlate with highly east-trending magnetic domains in detailed airborne magnetic surveys. At the outcrop scale, BIFs typically display very thin alternating laminae ranging from 1 to 6 mm (locally up to 15 mm). These laminae consist of chert, jasper, mudstone, greywacke and very fine grained magnetite±hematite (Figure GS2017-11-5d). Very fine grained biotite is concentrated in

the mudstone layers and imparts a unique brownish colour; the jasper layers are up to 1 cm thick. Layering in the BIFs locally displays mesoscopic Z-asymmetric folds and a penetrative foliation.

Thin beds of minor volcanic sedimentary rocks (subunit 3c) are present in the upper section of unit 3 and consist of volcanic mudstone and sandstone (Table GS2017-11-1). A section >1 m thick of this subunit is exposed west of Wasekwan Lake. A similar exposure of rocks, about 10 m in thickness, is observed in the Keewatin River area in the northern belt (Yang and Beaumont-Smith, 2015a).

#### **Pre-Sickle intrusive suite (units 4 and 5)**

Plutonic rocks in the pre-Sickle intrusive suite occur as intrusions or plutons that are emplaced into the Wasekwan group but overlain unconformably by the Sickle group (Gilbert

et al., 1980; Baldwin et al., 1987; Beaumont-Smith and Bohm, 2004). Unit 4 gabbro and unit 5 granitoid rocks, diorite, quartz diorite and minor gabbroic rocks are included in this suite (Table GS2017-11-1).

#### **Gabbro (unit 4)**

Gabbro of unit 4 is represented by the Cockeram Lake intrusion, which intrudes unit 2 and unit 1 in the northeastern to central part of the map area (Figure GS2017-11-2). The gabbro occurs as an elongated intrusion or a sill-like body occupying the core of a macroscopic  $F_2$  fold that trends in an east-northeast direction through the central portion of the map area; the gabbro is then cut by granitic intrusions. This gabbro weathers greenish grey and is dark greenish grey to dark grey on fresh surfaces. It is medium grained, equigranular, massive and moderately to locally strongly foliated. The gabbro consists of 40–45% plagioclase laths (1–3 mm), 55–60% amphibole (pseudomorphs after pyroxene), minor iron-oxide minerals, and trace pyrrhotite and chalcopyrite (Figure GS2017-11-6a). The edges of both plagioclase and amphibole crystals are diffuse due to chlorite and sericite alteration. This gabbro contains a greenschist-facies metamorphic assemblage (chlorite, actinolite, epidote and albite). Quartz veinlets and veins (~2–5 cm wide) are locally common along extensional fractures, and some of these veins contain pyrite and/or chalcopyrite.

The gabbro (unit 4) is petrologically similar to the Lynn Lake gabbro, which is dated at  $1871.3 \pm 2.4$  Ma by Turek et al. (2000) and hosts the past producing Ni-Cu mine (22.2 Mt of ore grading 1.0% Ni and 0.5% Cu).

#### **Granitoid rocks (subunit 5a)**

Granitoid plutons of the pre-Sickle intrusive suite (unit 5) are exposed in northern and southern parts of the map area (Figure GS2017-11-2), and include a variety of rock types, such as diorite, quartz diorite, tonalite, granodiorite, granite and associated pegmatitic and aplitic dikes, with minor gabbro. A tonalite sample of this suite at Norrie Lake was dated at  $1876 \pm 8/-6$  Ma by Baldwin et al. (1987) using zircon U-Pb geochronology. These intrusive rocks (Table GS2017-11-1) are divided into two subunits based on the field relations and rock types: tonalite, granodiorite and granite and associated pegmatitic and aplitic rocks (subunit 5a); and diorite, quartz diorite and minor gabbroic rocks (subunit 5b).

Subunit 5a granitoid rocks comprise tonalite, granodiorite and granite, and minor related pegmatitic and aplitic dikes. Granodiorite is the dominant phase of the Cockeram Lake pluton and intrudes subunits 2c and 2d (Figure GS2017-11-6b). The granodiorite is medium to coarse grained, massive, equigranular to locally porphyritic, and is weakly to moderately foliated. It weathers greyish pink to light beige and consists of 20–30% anhedral quartz, 25–35% subhedral plagioclase laths, 20–25% K-feldspar, 5–10% biotite ( $\pm$ hornblende) and accessory iron-oxide minerals. This mineral assemblage is consistent with I-type granite of Chappell and White (1974) or the magnetite-series granite of Ishihara (1981). Minor granite of subunit 5a is

differentiated from granodiorite by slightly higher K-feldspar and quartz content than the granodiorite. In places, medium- to coarse-grained granite dikes intrude unit 1 and are folded and foliated (Figure GS2017-11-6c). This granite is likely formed by differentiation of the same parent magma(s) and thus is considered part of the I-type and magnetite-series granites.

In the southern part of the map area, the supracrustal rocks of units 1 to 3 are cut by granitoid rocks ranging from tonalite to granodiorite to granite. The tonalite is fine to medium grained, grey to light grey, equigranular, moderately foliated and locally porphyritic. Its mineralogy consists of 15–25% quartz, 50–60% plagioclase, 15–20% amphibole and minor biotite, and is also characterized by chlorite and sericite alteration. At the contact zone, scattered disseminated pyrite is evident in the tonalite.

Pegmatite and/or aplite of unit 5a are more commonly associated with granite and granodiorite than with tonalite. They occur as dikes that are a few centimetres to a few metres wide and consist of quartz, feldspar and minor biotite ( $\pm$ muscovite).

#### **Diorite, quartz diorite and minor gabbroic rocks (subunit 5b)**

Diorite and quartz diorite (subunit 6b) mostly occur as marginal phases of the Cockeram Lake pluton in the northern part, and as a small stock exposed in the central part of the map area. Quartz diorite is medium to dark grey on weathered and fresh surfaces, fine to medium grained, massive, equigranular and moderately to strongly foliated. Locally, the quartz diorite is porphyritic, containing plagioclase phenocrysts up to 1 cm in a fine- to medium-grained groundmass (Figure GS2017-11-6d). It consists of 5–10% anhedral quartz, 50–60% plagioclase laths with diffuse grain boundaries, 20–30% hornblende and minor biotite. Contacts between quartz diorite, diorite, granodiorite and granite are not observed in the Wasekwan Lake area, but many outcrops in the northern belt show that similar quartz diorite (and diorite) is cut by granodiorite (Yang and Beaumont-Smith, 2015c).

Minor gabbroic dikes cutting the quartz diorite are assigned to subunit 6b, similar to those observed in the Farley Lake area in the northern belt of the LLGB (Yang and Beaumont-Smith, 2016a).

#### **Post-Sickle intrusive suite (unit 6)**

Post-Sickle intrusive rocks of unit 6 occur as an elongated stock exposed mainly in the central portion of the map area (Figure GS2017-11-2). This unit comprises two subunits (Table GS2017-11-1): granodiorite (subunit 6a) and granite (subunit 6b), defined by a domain of muted magnetic response in detailed airborne magnetic data. Granitic rocks at the contact zone consist of dikes and veins to veinlets cutting unit 2 basalt (Figure GS2017-11-6e), although the dikes do not display notable deformation. The unit 6 granitoid intrusion cuts the Cockeram Lake gabbro (unit 4) in the northern part of map area (Figure GS2017-11-2). Subunit 6a returned an age determined at  $1855.6 \pm 8.3$  Ma (Beaumont-Smith, unpublished data, 2006)

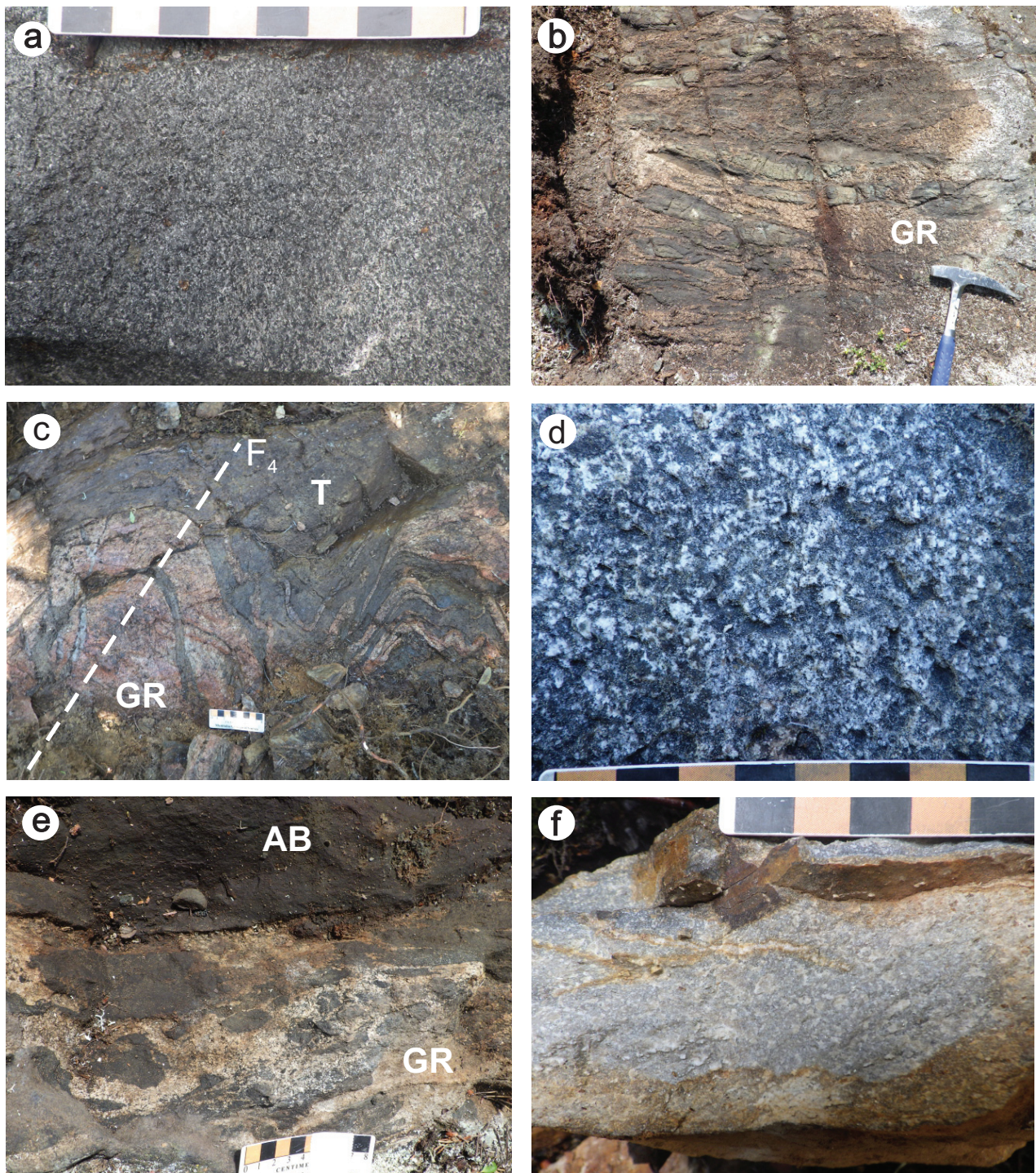


**Figure GS2017-11-6:** Outcrop photographs of map units 4, 5, 6 and 7 on PMAP2017-3 (Yang and Beaumont-Smith, 2017) in the Wasekwan Lake area: **a)** weakly foliated, massive, medium-grained, equigranular gabbro (unit 4; UTM Zone 14N, 387901E, 6296217N, NAD 83); **b)** dikes of medium grained, porphyritic to equigranular granodiorite (subunit 5a) intruding basalt of unit 2c at the contact zone (UTM 380752E, 6294014N); **c)** medium- to coarse-grained granite dikes cutting unit 1 intermediate tuff and folded by  $F_4$  fold that plunges  $045^\circ/57^\circ$  (subunit 5a; UTM 380238E, 6291506N); **d)** porphyritic quartz diorite with plagioclase phenocrysts up to 1 cm in a fine- to medium-grained groundmass (subunit 5b; UTM 379465E, 6294010N); **e)** medium-grained granodiorite (unit 6a) as veins and veinlets cutting strongly foliated basalt (subunit 2c; UTM 384451E, 6292943N); **f)** quartz-feldspar porphyry dike ~2 m wide, containing fine-grained pyrite disseminations, cutting unit 3 quartz feldspathic greywacke and unit 2 mafic volcanic rocks (subunit 7; UTM 383547E, 6291899N). Abbreviations: AB, aphanitic basalt; GR, granodiorite; T, mafic tuff.

by zircon U-Pb geochronology, which is within analytical uncertainties of the Burge Lake pluton ( $1857 \pm 2$  Ma; see Beaumont-Smith et al., 2006) in the northern belt. It is noted that the granodiorite and granite in the current map area correspond with magnetic lows, which is characteristic of reduced I-type and ilmenite-series granites (see Chappell and White, 1974; Ishihara, 1981) that may be associated with intrusion-related Au mineralization as reported elsewhere (e.g., Thorne et al., 2008; Yang et al., 2008).

The granodiorite of subunit 6b is pinkish on fresh surfaces and weathers beige to tan, is medium to coarse grained, foliated and equigranular to locally porphyritic. This granodiorite consists of 5–8% hornblende (partly altered to biotite), 3–5% discrete biotite flakes, 25–30% quartz, 30–40% plagioclase and 25–30% K-feldspar.

### **Late intrusive suite (unit 7)**

Unit 7 quartz-feldspar porphyry, pegmatite and/or aplite occur mostly as dikes in the southwestern and central portions of the map area (Figure GS2017-11-2). These dikes tend to be isolated, relatively lesser deformed and are not able to trace back to any plutons nearby on the surface. Their association with the pre- and post-Sickle intrusive suites (unit 5 and unit 6, respectively) is unknown. At the Central Manitoba Au occurrence, a quartz-feldspar porphyry dike, 2–3 m in thickness, cutting unit 3 greywacke and unit 2 mafic volcanic rocks contains pyrite ( $\pm$ arsenopyrite?; Figure GS2017-11-6f). The age of the dike was determined at  $1814 \pm 15$  Ma by zircon U-Pb geochronology (Jones, 2005; C.J. Beaumont-Smith, unpublished data, 2006), revealing that it is much younger than the granitic rocks from unit 5 pre-Sickle and unit 6 post-Sickle intrusive suites.

Unit 7 pegmatite and aplite commonly have muscovite ( $\pm$ tourmaline) in addition to biotite; this indicates that they are less likely to be related to I-type or magnetite-series granitoid rocks of both the pre-Sickle and post-Sickle intrusive suites, both of which typically lack muscovite.

### **Tectonite (unit 8)**

Tectonite of unit 8 comprises mylonitic mafic to felsic rocks within the JSZ (Figure GS2017-11-2) characterized by intense transposition and the development of  $S_2$  tectonic fabric. The protoliths of such high-strain rocks are difficult to determine in the field, although feldspar and quartz relicts may be partly preserved in felsic tectonite. Mafic tectonite derived from lava flows and/or volcanoclastic rocks are indistinguishable, in particular, those that are altered to very fine grained chlorite and sericite. In some cases, the tectonite shows evidence of multiple deformation events (Figure GS2017-11-7a). Quartz-carbonate ( $\pm$ pyrite) veins or veinlets occur in tectonite, and are primarily concentrated along the  $S_2$  foliation.

## **Structural geology**

Structural geology has been extensively investigated at both regional and deposit scales in the LLGB (Gilbert et al.,

1980; Gilbert, 1993; Peck et al., 1998; Beaumont-Smith and Rogge, 1999; Beaumont-Smith and Edwards, 2000; Beaumont-Smith et al., 2000; Ma et al., 2000; Anderson and Beaumont-Smith, 2001; Ma and Beaumont-Smith, 2001; Beaumont-Smith et al., 2001; Park et al., 2002; Beaumont-Smith and Böhm, 2002, 2003, 2004; Jones, 2005; Jones et al., 2006; Yang and Beaumont-Smith, 2015a, 2016a). Beaumont-Smith and Böhm (2002, 2004) defined as many as six deformation events ( $D_1$  to  $D_6$ ) in the LLGB. Although not all deformation fabrics are observed in the Wasekwan Lake area, this report follows the terms used by Beaumont-Smith and Böhm (2002, 2004) to describe the characteristics of the  $D_1$  to  $D_6$  structures. The  $D_1$  deformation is interpreted to be related to the assembly of volcanic terranes comprising the LLGB, but these fabrics and structures are mostly obscured by later deformation.

In the Wasekwan Lake area,  $D_2$  structures are the most penetrative and manifest as a steeply north-dipping  $S_2$  foliation and tight to isoclinal folds ( $F_2$ ) that have shallowly plunging hinges and associated minor chevron folds. Ductile shear zones that generally define unit contacts are thought to be related to  $D_2$  deformation, as the intensity of  $S_2$  fabrics and tightness of  $F_2$  folds increase toward contacts. The  $D_2$  shear zones are characterized by dextral shear-sense indicators on horizontal surfaces and steeply plunging, generally down-dip to slightly oblique (easterly pitch) stretching lineations. The structural geometry of the Wasekwan Lake area is characterized by shallowly plunging  $F_2$  fold axes, which steepen to subvertical within  $D_2$  shear zones.

The JSZ, a regional east–west trending shear zone, transects the southern part of the map area (Figure GS2017-11-2) and can be traced over 100 km along strike. The JSZ is a protracted and dominantly dextral transpressional fault zone (Beaumont-Smith and Rogge, 1999; Jones, 2005; Jones et al., 2006). Numerous dextral shear sense indicators are observed on the horizontal surface within the JSZ. The development of narrow zones of shallowly plunging stretching lineations in the core of the shear zone reflects kinematics consistent with shear-zone development in response to dextral transpression.

The fabrics of  $D_3$  deformation are represented by close to tight, S-asymmetric  $F_3$  folds and northwest-trending, axial-planar  $S_3$  crenulation cleavages in the map area (Figure GS2017-11-7b). Also,  $F_4$  folds are pervasive throughout the map area. These folds plunge steeply to the northeast and are associated with steeply dipping, northeast-striking, axial-planar  $S_4$  crenulation cleavages. Mesoscopic structures associated with  $D_5$  deformation include open  $F_5$  conjugate folds, kink bands and crenulations, and a brittle  $D_5$  fault (Figure GS2017-11-7c). The post-mineralization ‘T1 fault’ at the BT mine open pit (Peck et al., 1998; Figure GS2017-11-2) is most likely a  $D_5$  structure.

The  $D_6$  deformation was brittle to ductile, represented by sinistral reactivation of  $D_2$  shear zones (Beaumont-Smith and Böhm, 2004). In places, retrograde actinolite crystals up to 1.5 cm (Figure GS2017-11-7d) are randomly oriented on the planes of associated planar structures (cleavages, fractures).

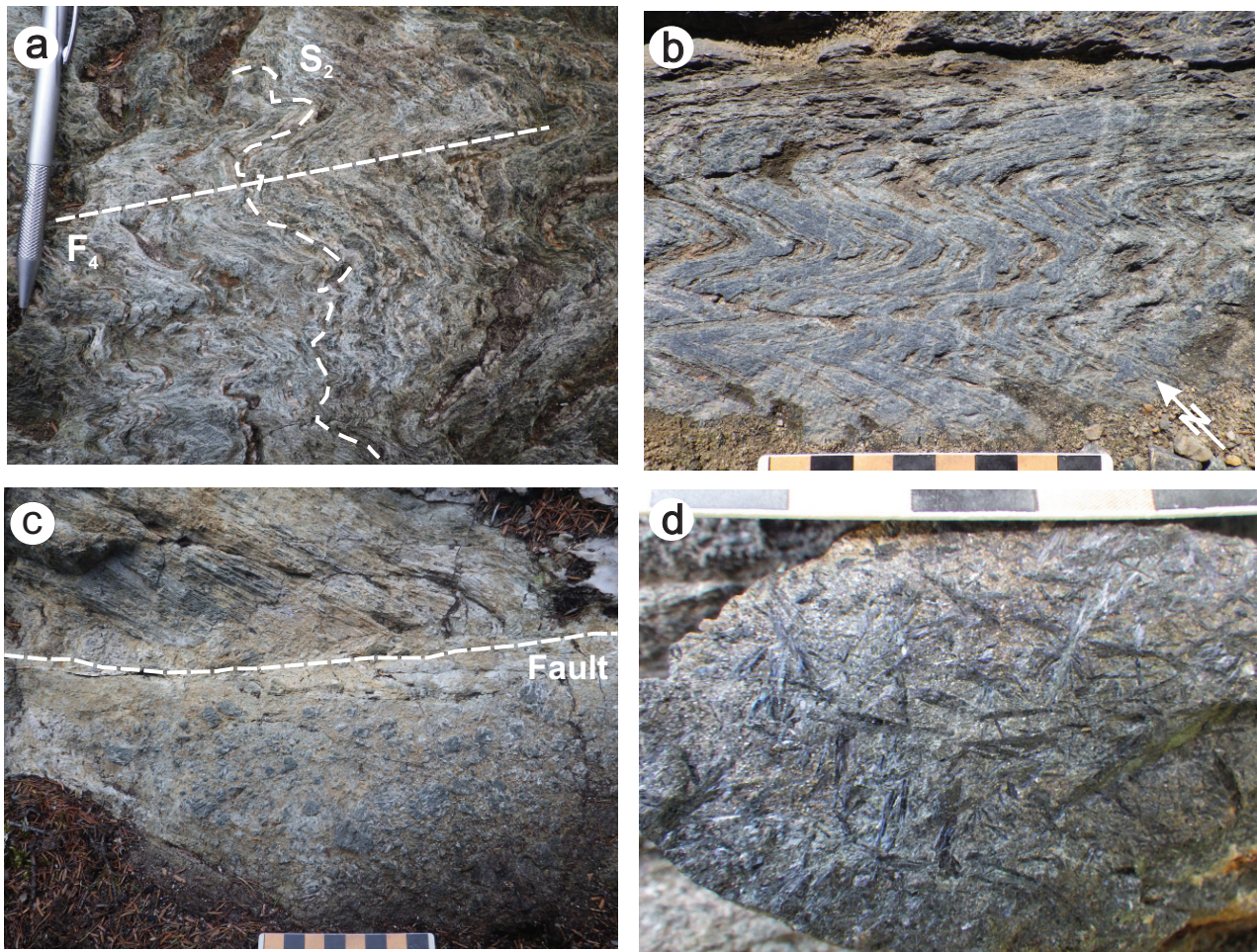


**Figure GS2017-11-7:** Outcrop photographs of map unit 7 tectonite, structural features and retrograde metamorphic rocks on PMAP2017-3 (Yang and Beaumont-Smith, 2017) in the Wasekwan Lake area: **a)** mafic tectonite showing  $S_2$  foliation and associated quartz veins folded by  $F_4$  folds (UTM Zone 14N, 383945E, 6291623N, NAD 83); **b)**  $F_3$  fold vertically plunging to the northwest within the Johnson shear zone (UTM 385018E; 6291878N); **c)** drag-folding along hangingwall contact of a brittle fault ( $215^\circ/35^\circ$ ), which is related to  $D_5$  deformation and cuts unit 1a felsic volcanic rock and actinolite alteration, suggests reverse movement (UTM 380159N, 6291960N); **d)** randomly oriented acicular actinolite crystals related to retrograde metamorphism (UTM 381326E, 6292353N).

## Economic considerations

The presence of significant Au mineralization at the BT deposit and Linkwood property along or adjacent to the JSZ demonstrates the economic potential of this long-lived structure in the Wasekwan Lake area. The BT open-pit operation produced 2457 kg (79 000 oz.) of Au from 1993 to 1996 (Richardson et al., 1996; Jones et al., 2006). Puritch et al. (2012) estimated that remaining mineral resources at the BT deposit are 1.021 Mt grading 1.4 g/t Au (45 000 oz. in the indicated category) and 2.344 Mt grading 1.04 g/t Au (78 500 oz. in the inferred category). Noteworthy is the Linkwood Au property, located approximately 3.5 km west-northwest of the BT mine, which also contains a significant mineral resource, with 30.84 Mt grading 1.16 g/t Au in both indicated and inferred categories (~820 000 oz. Au; see Puritch et al., 2013). Old trenches expose part of the Central Au occurrence, 1 km west of the BT mine, where Au is hosted in a quartz-feldspar porphyry. A surface grab sample returned 4.5 g/t Au (Bateman, 1945; Ferreira and

Baldwin, 1997), whereas two feldspar porphyry samples yielded 1.45 and 3.15 g/t Au, respectively (Jones et al., 2006).

New mapping suggests that rheological differences between volcanoclastic rocks (unit 1), Fe-rich mafic volcanic rocks (unit 2) and sedimentary rocks (unit 3) acted as foci for ductile strain during multiple phases of deformation along the JSZ (and associated subsidiary  $D_2$  structures), focusing Au-bearing fluids into structural and chemical traps. Potential structural traps include areas where  $D_2$  shear zones and  $D_3$  and  $D_4$  fabrics intersect as these may locally form dilatant zones. The sources of auriferous fluids are the subject of ongoing collaborative research between the Manitoba Geological Survey and the Geological Survey of Canada.

Jones et al. (2006) noted that Au-bearing quartz-sulphide veins are hosted in granitoid intrusions and dikes that are rheologically more competent than the surrounding mafic volcanic and volcanoclastic rocks. Gold-bearing (pyrite+galena) quartz veins also cut deformed quartz-feldspar porphyry at the

Bonanza deposit approximately 12 km east of the BT deposit (Peck, 1985; Jones et al., 2006; Figure GS2017-11-1). Ten kilometres east of the BT deposit, the Esker Au showing consists of pyrite- and chalcopyrite-bearing quartz veins cutting variably foliated granodiorite (Jones et al., 2006; Figure GS2017-11-1). Interestingly, Jones et al. (2006) point out that high-grade mineralized zones (up to 120 g/t Au) in the BT deposit are locally associated with folded and boudinaged quartz-pyrite veins hosted in carbonate- and sericite-altered feldspar porphyry dikes that cut the shear zone. Such observations suggest that quartz-pyrite vein systems hosted in granitic intrusions of the post-Sickle intrusive suite (unit 6) and late intrusive suite (unit 7) are potentially an important Au-exploration target in the region.

The unit 4 gabbro intrusions are saturated with sulphides (e.g., Cockeram Lake intrusion), and are petrologically similar to the Lynn Lake gabbro intrusion that hosts the Lynn Lake Ni-Cu-Co deposit, which suggests that these intrusions may also have potential for magmatic Ni-Cu-Co ( $\pm$ PGE). In addition, relatively oxidized I-type granitoid intrusions of unit 5 may have potential for porphyry Cu-Au (Mo) mineralization, but more work is required to look into the emplacement depth of these granitoid intrusions (e.g., Yang, 2017) and their petrogenetic types (e.g., Chappell and White, 1974; Ishihara, 1981) to fully assess their mineral potential.

## Acknowledgments

The authors thank J. Watts for providing enthusiastic and capable field assistance, E. Anderson and N. Brandson for thorough logistical support. Thanks go to Carlisle Goldfields Ltd. and Alamos Gold Inc. for providing detailed airborne geophysical data and LiDAR (light detection and ranging) data. This study benefited from discussions with M. Rein (Alamos Gold Inc.), C. Lawley (Geological Survey of Canada) and S.D. Anderson in the field. Thanks go to P. Lenton and G. Keller for technical support; L. Chackowsky and B. Lenton for providing GIS data, digitizing map data and drafting figures; M. Pacey for assembling the digital database for a hand-held data acquisition system; and C. Epp for cataloguing, processing and preparing the samples. The manuscript benefited greatly from constructive reviews by K.D. Reid and S.D. Anderson, and from technical editing by M.-F. Dufour.

## References

- Anderson, S.D. and Beaumont-Smith, C.J. 2001: Structural analysis of the Pool Lake–Boiley Lake area, Lynn Lake greenstone belt (NTS 64C/11); *in* Report of Activities 2001, Manitoba Industry, Trade and Mines, Manitoba Geological Survey, p. 76–85.
- Ansdeell, K.M. 2005: Tectonic evolution of the Manitoba-Saskatchewan segment of the Paleoproterozoic Trans-Hudson Orogen, Canada; *Canadian Journal of Earth Sciences*, v. 42, p. 741–759.
- Ansdeell, K.M., Corrigan, D., Stern, R. and Maxeiner, R. 1999: SHRIMP U-Pb geochronology of complex zircons from Reindeer Lake, Saskatchewan: implications for timing of sedimentation and metamorphism in the northwestern Trans-Hudson Orogen; Geological Association of Canada–Mineralogical Association of Canada, Joint Annual Meeting, Program with Abstracts, v. 24, p. 3.
- Baldwin, D.A., Syme, E.C., Zwanzig, H.V., Gordon, T.M., Hunt, P.A. and Stevens, R.P. 1987: U-Pb zircon ages from the Lynn Lake and Rusty Lake metavolcanic belts, Manitoba: two ages of Proterozoic magmatism; *Canadian Journal of Earth Sciences*, v. 24, p. 1053–1063.
- Baragar, W.R.A., Ernst, R.E., Hulbert, L. and Peterson, T. 1996: Longitudinal petrochemical variation in the Mackenzie dyke swarm, northwestern Canadian Shield; *Journal of Petrology*, v. 37, p. 317–359.
- Bateman, J.D. 1945: McVeigh Lake area, Manitoba; Geological Survey of Canada, Paper 45-14, 34 p.
- Beaumont-Smith, C.J. 2008: Geochemistry data for the Lynn Lake greenstone belt, Manitoba (NTS 64C11-16); Manitoba Science, Technology, Energy and Mines, Manitoba Geological Survey, Open File OF2007-1, 5 p.
- Beaumont-Smith, C.J. and Böhm, C.O. 2002: Structural analysis and geochronological studies in the Lynn Lake greenstone belt and its gold-bearing shear zones (NTS 64C10, 11, 12, 14, 15 and 16), Manitoba; *in* Report of Activities 2002, Manitoba Industry, Trade and Mines, Manitoba Geological Survey, p. 159–170.
- Beaumont-Smith, C.J. and Böhm, C.O. 2003: Tectonic evolution and gold metallogeny of the Lynn Lake greenstone belt, Manitoba (NTS 64C10, 11, 12, 14, 15 and 16), Manitoba; *in* Report of Activities 2003, Manitoba Industry, Economic Development and Mines, Manitoba Geological Survey, p. 39–49.
- Beaumont-Smith, C.J. and Böhm, C.O. 2004: Structural analysis of the Lynn Lake greenstone belt, Manitoba (NTS 64C10, 11, 12, 14, 15 and 16); *in* Report of Activities 2004, Manitoba Industry, Economic Development and Mines, Manitoba Geological Survey, p. 55–68.
- Beaumont-Smith, C.J. and Edwards, C.D. 2000: Detailed structural analysis of the Johnson shear zone in the west Gemmill Lake area (NTS 64C/11); *in* Report of Activities 2000, Manitoba Industry, Trade and Mines, Manitoba Geological Survey, p. 64–67.
- Beaumont-Smith, C.J. and Rogge, D.M. 1999: Preliminary structural analysis and gold metallogeny of the Johnson shear zone, Lynn Lake greenstone belt (parts of NTS 64C/10, 11, 15); *in* Report of Activities 1999, Manitoba Energy and Mines, Geological Services, p. 61–66.
- Beaumont-Smith, C.J., Anderson, S.D. and Böhm, C.O. 2001: Structural analysis and investigations of shear-hosted gold mineralization in the southern Lynn Lake greenstone belt (parts of NTS 64C/11, /12, /15, /16); *in* Report of Activities 2001, Manitoba Industry, Trade and Mines, Manitoba Geological Survey, p. 67–75.
- Beaumont-Smith, C.J., Lentz, D.R. and Tweed, E.A. 2000: Structural analysis and gold metallogeny of the Farley Lake gold deposit, Lynn Lake greenstone belt (NTS 64C/16); *in* Report of Activities 2000, Manitoba Industry, Trade and Mines, Manitoba Geological Survey, p. 73–81.
- Beaumont-Smith, C.J., Machado, N. and Peck, D.C. 2006: New uranium-lead geochronology results from the Lynn Lake greenstone belt, Manitoba (NTS 64C11-16); Manitoba Science, Technology, Energy and Mines, Manitoba Geological Survey, Geoscientific Paper GP2006-1, 11 p.
- Chappell, B.W. and White, A.J.R. 1974: Two contrasting granite types; *Pacific Geology*, v. 8, p. 173–174.
- Corrigan, D., Galley, A.G. and Pehrsson, S. 2007: Tectonic evolution and metallogeny of the southwestern Trans-Hudson Orogen; *in* Mineral Deposits of Canada: A Synthesis of Major Deposit-Types, District Metallogeny, the Evolution of Geological Provinces, and Exploration Methods, W.D. Goodfellow (ed.), Geological Association of Canada, Mineral Deposits Division, Special Publication 5, p. 881–902.
- Corrigan, D., Pehrsson, S., Wodicka, N. and de Kemp, E. 2009: The Palaeoproterozoic Trans-Hudson Orogen: a prototype of modern accretionary processes; *in* Ancient Orogens and Modern Analogues, J.B. Murphy, J.D. Keppie, and A.J. Hynes (ed.), Geological Society of London, Special Publications, v. 327, p. 457–479.

- Fedikow, M.A.F. 1986: Geology of the Agassiz stratabound Au-Ag deposit, Lynn Lake, Manitoba; Manitoba Energy and Mines, Geological Services, Open File Report OF85-5, 80 p.
- Fedikow, M.A.F. 1992: Rock geochemical alteration studies at the MacLellan Au-Ag deposit, Lynn Lake, Manitoba; Manitoba Energy and Mines, Geological Services, Economic Geology Report ER92-1, 237 p.
- Fedikow, M.A.F. and Gale, G.H. 1982: Mineral deposit studies in the Lynn Lake area; *in* Report of Field Activities 1982, Manitoba Department of Energy and Mines, Mineral Resources Division, p. 44–54.
- Ferreira, K.J. and Baldwin, D.A. 1997: Mineral deposits and occurrences in the Cockeram Lake area, NTS 64C/15; Manitoba Energy and Mines, Geological Services, Mineral Deposit Series Report No. 8, 154 p.
- Gilbert, H.P. 1993: Geology of the Barrington Lake–Melvin Lake–Fraser Lake area; Manitoba Energy and Mines, Geological Services, Geological Report GR87-3, 97 p.
- Gilbert, H.P., Syme, E.C. and Zwanzig, H.V. 1980: Geology of the metavolcanic and volcanoclastic metasedimentary rocks in the Lynn Lake area; Manitoba Energy and Mines, Mineral Resources Division, Geological Paper GP80-1, 118 p.
- Hoffman, P.H. 1988: United plates of America, the birth of a craton: Early Proterozoic assembly and growth of Laurentia; *Annual Reviews of Earth and Planetary Sciences*, v. 16, p. 543–603.
- Ishihara, S. 1981: The granitoid series and mineralization; *Economic Geology*, 75<sup>th</sup> Anniversary Volume, p. 458–484.
- Jones, L.R. 2005: Geology of the shear-hosted Burnt Timber deposit, Lynn, northern Manitoba; M.Sc. thesis, Laurentian University, Sudbury, Ontario, 63 p.
- Jones, L.R., Lafrance, B. and Beaumont-Smith, C.J. 2006: Structural controls on gold mineralization at the Burnt Timber Mine, Lynn Lake Greenstone Belt, Trans-Hudson Orogen, Manitoba; *Exploration and Mining Geology*, v. 15, p. 89–100.
- Jurkowski, J.S. 1999: Uranium-lead geochronology study of Lynn Lake greenstone belt, Manitoba; M.Sc. thesis, University of Windsor, Windsor, Ontario, 95 p.
- Lewry, J.F. and Collerson, K.D. 1990: The Trans-Hudson Orogen: extent, subdivisions and problems; *in* The Early Proterozoic Trans-Hudson Orogen of North America, J.F. Lewry and M.R. Stauffer (ed.), Geological Association of Canada, Special Paper 37, p. 1–14.
- Ma, G. and Beaumont-Smith, C.J. 2001: Stratigraphic and structural mapping of the Agassiz Metaltect near Lynn Lake, Lynn Lake greenstone belt (parts of NTS 64C/14, /15); *in* Report of Activities 2001, Manitoba Industry, Trade and Mines, Manitoba Geological Survey, p. 86–93.
- Ma, G., Beaumont-Smith, C.J. and Lentz, D.R. 2000: Preliminary structural analysis of the Agassiz Metaltect near the MacLellan and Dot lake gold deposits, Lynn Lake greenstone belt (parts of NTS 64C/14, /15); *in* Report of Activities 2000, Manitoba Industry, Trade and Mines, Manitoba Geological Survey, p. 51–56.
- Manitoba Energy and Mines 1986: Granville Lake, NTS 64C; Manitoba Energy and Mines, Minerals Division, Bedrock Geology Compilation Map Series, Map 64C, scale 1:250 000.
- Milligan, G.C. 1960: Geology of the Lynn Lake district; Manitoba Department of Mines and Natural Resources, Mines Branch, Publication 57-1, 317 p.
- Norman, G.W.H. 1933: Granville Lake district, northern Manitoba; Geological Survey of Canada, Summary Report, Part C, p. 23–41.
- Park, A.F., Beaumont-Smith, C.J. and Lentz, D.R. 2002: Structure and stratigraphy in the Agassiz Metaltect, Lynn Lake greenstone belt (NTS 64C/14 and /15), Manitoba; *in* Report of Activities 2002, Manitoba Industry, Trade and Mines, Manitoba Geological Survey, p. 171–186.
- Peck, D.C., 1985, Geological investigations at Cartwright Lake, Manitoba; Manitoba Energy and Mines, Geological Services, *in* Report of Field Activities 1985, p. 37–40.
- Peck, D.C. and Smith, T.E, 1989: The geology and geochemistry of an Early Proterozoic volcanic-arc association at Cartwright Lake: Lynn Lake greenstone belt, northwestern Manitoba; *Canadian Journal of Earth Sciences*, v. 26, p. 716–736.
- Peck, D.C., Lin, S., Atkin, K. and Eastwood, A.M. 1998: Reconnaissance structural studies of Au metaltects in the Lynn Lake greenstone belt (parts of NTS 63C/10, C/11, C/15); *in* Report of Activities 1998, Manitoba Energy and Mines, Geological Services, p. 69–74.
- Pinsent, R.H. 1980: Nickel-copper mineralization in the Lynn Lake gabbro; Manitoba Energy and Mines, Geological Services, Economic Geology Report ER79-3, 138 p.
- Puritch, E., Burga, D. and Wu, Y. 2012: Technical report and resource estimate on the Burnt Timber property, Lynn Lake, Northern Manitoba, Canada; NI-43-101 & 43-101F1, P & E Mining Consultants Inc., Technical Report No. 248, 96 p.
- Puritch, E., Burga, D. and Wu, Y. 2013: Technical report and resource estimate on the Linkwood property, Lynn Lake, Northern Manitoba, Canada; NI-43-101 & 43-101F1, P & E Mining Consultants Inc., Technical Report No. 252, 80 p.
- Richardson, D.J., Ostry, G., Weber, W. and Fogwill, W.D. 1996: Gold deposits of Manitoba; Manitoba Energy and Mines, Economic Geology Report ER86-1 (2<sup>nd</sup> Edition), 114 p.
- Stauffer, M.R. 1984: Manikewan: an Early Proterozoic ocean in central Canada, its igneous history and orogenic closure; *Precambrian Research*, v. 25, p. 257–281.
- Stern, R.A., Syme, E.C. and Lucas, S.B. 1995: Geochemistry of 1.9 Ga MORB- and OIB-like basalts from the Amisk collage, Flin Flon Belt, Canada: evidence for an intra-oceanic origin; *Geochimica et Cosmochimica Acta*, v. 59, p. 3131–3154.
- Syme, E.C. 1985: Geochemistry of metavolcanic rocks in the Lynn Lake Belt; Manitoba Energy and Mines, Geological Services/Mines Branch, Geological Report GR84-1, 84 p.
- Thorne, K.G., Lentz, D.R., Hoy, D., Fyffe, L.R. and Cabri, L.J. 2008: Characteristics of mineralization at the Main Zone of the Clarence Stream Gold Deposit, southwestern New Brunswick, Canada: evidence for an intrusion-related gold system in the northern Appalachian Orogen; *Exploration and Mining Geology*, v. 17, p. 13–49.
- Turek, A., Woodhead, J. and Zwanzig H.V. 2000: U-Pb age of the gabbro and other plutons at Lynn Lake (part of NTS 64C); *in* Report of Activities 2000, Manitoba Industry, Trade and Mines, Manitoba Geological Survey, p. 97–104.
- Yang, X.M. 2017: Estimation of crystallization pressure of granite intrusions; *Lithos*, v. 286–287, p. 324–329.
- Yang, X.M. and Beaumont-Smith, C.J. 2015a: Geological investigations of the Keewatin River area, Lynn Lake greenstone belt, northwestern Manitoba (parts of NTS 64C14, 15); *in* Report of Activities 2015, Manitoba Mineral Resources, Manitoba Geological Survey, p. 52–67.
- Yang, X.M. and Beaumont-Smith, C.J. 2015b: Bedrock geology of the Keewatin River area, Lynn Lake greenstone belt, northwestern Manitoba (parts of NTS 64C14, 15); Manitoba Mineral Resources, Manitoba Geological Survey, Preliminary Map PMAP2015-3, scale 1:20 000.
- Yang, X.M. and Beaumont-Smith, C.J. 2015c: Granitoid rocks in the Lynn Lake region, northwestern Manitoba: preliminary results of reconnaissance mapping and sampling; *in* Report of Activities 2015, Manitoba Mineral Resources, Manitoba Geological Survey, p. 68–78.

- Yang, X.M. and Beaumont-Smith, C.J. 2016a: Geological investigations in the Farley Lake area, Lynn Lake greenstone belt, northwestern Manitoba (part of NTS 64C16); *in* Report of Activities 2016, Manitoba Growth, Enterprise and Trade, Manitoba Geological Survey, p. 99-114.
- Yang, X.M. and Beaumont-Smith, C.J. 2016b: Bedrock geology of the Farley Lake area, Lynn Lake greenstone belt, northwestern Manitoba (part of NTS 64C16); Manitoba Growth, Enterprise and Trade, Manitoba Geological Survey, Preliminary Map PMAP2016-5, scale 1:20 000.
- Yang, X.M. and Beaumont-Smith, C.J. 2017: Bedrock geology of the Wasekwan Lake area, Lynn Lake greenstone belt, northwestern Manitoba (parts of NTS 64C10, 15); Manitoba Growth, Enterprise and Trade, Manitoba Geological Survey, Preliminary Map PMAP2017-3, scale 1:20 000.
- Yang, X.M., Lentz, D.R., Chi, G. and Thorne, K.G. 2008: Geochemical characteristics of gold-related granitoids in southwestern New Brunswick, Canada; *Lithos*, v. 104, p. 355–377.
- Zwanzig, H.V. 2000: Geochemistry and tectonic framework of the Kisseynew Domain–Lynn Lake belt boundary (part of NTS 63P/13); *in* Report of Activities 2000, Manitoba Industry, Trade and Mines, Manitoba Geological Survey, p. 91–96.
- Zwanzig, H.V., Syme, E.C. and Gilbert, H.P. 1999: Updated trace element geochemistry of ca. 1.9 Ga metavolcanic rocks in the Paleoproterozoic Lynn Lake belt; Manitoba Industry, Trade and Mines, Geological Services, Open File Report OF99-13, 46 p.